6. J. Garthwaite, S. L. Charles, R. Chess-Williams, *Nature* **336**, 385 (1988); D. S. Bredt and S. H. Snyder, *Proc. Natl. Acad. Sci. U.S.A.* **86**, 9030 (1989).
7. I. Ahmad *et al.*, *Neuron* **12**, 155 (1994).
8. J. A. Connor, *Proc. Natl. Acad. Sci. U.S.A.* **83**, 6179 (1986); M. P. Mattson and S. B. Kater, *J. Neurosci.* **7**, 4034 (1987).
9. G. A. Bohme, C. Bon, J. Stutzmann, A. Doble, J. Blanchard, *Eur. J. Pharmacol.* **199**, 379 (1991); T. J. O'Dell, R. D. Hawkins, E. R. Kandel, O. Arancio, *Proc. Natl. Acad. Sci. U.S.A.* **88**, 11285 (1991); E. M. Schuman and D. V. Madison, *Science* **254**, 1503 (1991); J. E. Haley, G. L. Wilcox, P. F. Chapman, *Neuron* **8**, 211 (1992); M. Zhuo, S. A. Small, E. R. Kandel, R. D. Hawkins, *Science* **260**, 1946 (1993).
10. C. V. Williams, D. Nordquist, S. C. McLoon, *J. Neurosci.* **14**, 1746 (1994).
11. G. Prusky, M. Hofer, M. Constantine-Paton, *Soc. Neurosci. Abstr.* **18**, 1311 (1992).
12. S. C. McLoon and R. D. Lund, *Exp. Brain Res.* **45**, 277 (1982); D. D. M. O'Leary, C. R. Gerfen, W. M. Cowan, *Dev. Brain Res.* **10**, 93 (1983); S. Thanos and F. Bonhoeffer, *J. Comp. Neurol.* **224**, 407 (1984).
13. C. V. Williams and S. C. McLoon, *J. Neurosci.* **11**, 445 (1991).
14. S. Moncada, R. M. J. Palmer, E. A. Higgs, *Pharmacol. Rev.* **43**, 109 (1991).
15. Drugs were dissolved in saline at the stated concentrations and administered in 150-μl drops to the chorioallantoic membrane of chick embryos daily.
16. M. A. Dwyer, D. S. Bredt, S. H. Snyder, *Biochem. Biophys. Res. Commun.* **176**, 1136 (1991); C. Iadecola, X. Xu, F. Zhang, J. Hu, E. E. El-Fakahany, *Neurochem. Res.* **19**, 501 (1994).
17. V. Hamburger and H. L. Hamilton, *J. Morphol.* **88**, 49 (1951).
18. K. Tanaka *et al.*, *Neurosci. Lett.* **127**, 129 (1991).
19. J. H. Sandell, *J. Comp. Neurol.* **238**, 466 (1985); T. M. Dawson, D. S. Bredt, M. Fotuhi, P. M. Hwang, S. H. Snyder, *Proc. Natl. Acad. Sci. U.S.A.* **88**, 7797 (1991).
20. H. H. Wu and S. C. McLoon, *Soc. Neurosci. Abstr.*, in press.
21. S. C. McLoon, *Science* **215**, 1418 (1982).
22. L. Galli and L. Maffei, *ibid.* **242**, 90 (1988); L. Maffei and L. Galli-Resta, *Proc. Natl. Acad. Sci. U.S.A.* **87**, 2861 (1990); M. Meister, R. O. L. Wong, D. A. Baylor, C. J. Shatz, *Science* **252**, 939 (1991).
23. L. Nowak, P. Bregestovaki, P. Ascher, A. Herbet, A. Prochiantz, *Nature* **307**, 462 (1984); M. L. Mayer, G. L. Westbrook, P. B. Guthrie, *ibid.* **309**, 261 (1984).
24. M. L. Mayer and G. L. Westbrook, *J. Physiol. (London)* **361**, 65 (1985); C. E. Jahr and C. F. Stevens, *Nature* **325**, 522 (1987); P. Ascher, P. Bregestovski, L. Nowak, *J. Physiol. (London)* **399**, 207 (1988).
25. D. S. Bredt and S. H. Snyder, *Proc. Natl. Acad. Sci. U.S.A.* **87**, 682 (1990).
26. R. A. Nichols, T. S. Sihra, A. J. Czernik, A. C. Nairn, P. Greengard, *Nature* **343**, 647 (1990); G. Lonart, J. Wang, K. M. Johnson, *Eur. J. Pharmacol.* **220**, 271 (1992); P. R. Montague, C. D. Gancayco, M. J. Winn, R. B. Marchase, M. J. Friedlander, *Science* **263**, 973 (1994).
27. P. G. Nelson, C. Yu, R. D. Fields, E. A. Neale, *Science* **244**, 585 (1989); R. D. Fields, E. A. Neale, P. G. Nelson, *J. Neurosci.* **10**, 2950 (1990).
28. We thank E. El-Fakahany and J. Hu for assistance with the NOS assay, G. Wilcox for discussions on the use of the drugs, L. McLoon and D. Nordquist for critical comments on the manuscript, and D. Waid and B. McAdams for technical advice. Supported by grants EY05371 and EY07133 from the National Eye Institute of the National Institutes of Health.

21 December 1993; accepted 15 June 1994

Activation of the Sphingomyelin Cycle Through the Low-Affinity Neurotrophin Receptor

Rick T. Dobrowsky, Mark H. Werner, Alexander M. Castellino, Moses V. Chao, Yusuf A. Hannun*

The role of the low-affinity neurotrophin receptor ($p75^{NTR}$) in signal transduction is undefined. Nerve growth factor can activate the sphingomyelin cycle, generating the putative-lipid second messenger ceramide. In T9 glioma cells, addition of a cell-permeable ceramide analog mimicked the effects of nerve growth factor on cell growth inhibition and process formation. This signaling pathway appears to be mediated by $p75^{NTR}$ in T9 cells and NIH 3T3 cells overexpressing $p75^{NTR}$. Expression of an epidermal growth factor receptor–$p75^{NTR}$ chimera in T9 cells imparted to epidermal growth factor the ability to activate the sphingomyelin cycle. These data demonstrate that $p75^{NTR}$ is capable of signaling independently of the *trk* neurotrophin receptor ($p140^{trk}$) and that ceramide may be a mediator in neurotrophin biology.

Nerve growth factor (NGF) controls the survival, development, and differentiation of neurons of the peripheral and central nervous systems (*1*) and interacts with two classes of binding sites. The high-affinity binding site ($K_d \sim 10^{-11}$ M) requires expression of the product of the *trk* proto-oncogene, $p140^{trk}$, which is a receptor tyrosine kinase (*2*, *3*). The low-affinity NGF receptor ($K_d \sim 10^{-9}$ M) is a highly glycosylated, 75-kD transmembrane protein that lacks kinase activity (*4*) and is termed $p75^{NTR}$ (*5*). Although $p140^{trk}$ can mediate NGF-induced effects in the absence of $p75^{NTR}$ (*6*), the functional significance of $p75^{NTR}$ in NGF signal transduction is unresolved. This uncertainty is due, in part, to the lack of evidence coupling $p75^{NTR}$ to activation of signal transduction pathways. Cytokines such as tumor necrosis factor–α (TNF-α) (*7*) or interleukin-1β (*8*) have been shown to activate the sphingomyelin (SM) cycle in a proposed signaling pathway (*7*, *9*). The activation of the SM cycle by ligands that inhibit cell growth and induce differentiation (*10*) led to the hypothesis that some of the effects of NGF may be associated with activation of SM hydrolysis. Moreover, the structural homology between $p75^{NTR}$ and TNF-α receptors (*11*) suggested that NGF might activate the SM cycle through $p75^{NTR}$. We therefore examined the effects of NGF on the SM cycle and the role of $p75^{NTR}$ in this process.

Rat T9 anaplastic glioblastoma cells undergo growth inhibition and differentiation to an astrocyte-like phenotype in response to NGF (*12*). Similar to NGF, the cell-permeable ceramide analog, C_2-ceramide (*13*), induced a dose-dependent decrease in the uptake of [^{3}H]thymidine (Fig. 1). This effect appears to result from growth inhibition and not toxicity because more than 90% of the cells remained viable as determined by exclusion of trypan blue. Similarly, C_2-ceramide also mimicked the effect of NGF on T9 cell morphology and doubled the percentage of cells bearing processes greater than one cell body in diameter (Fig. 2, A and B). To determine if ceramide may be an endogenous mediator, we investigated the effect of NGF on the activation of the SM cycle in T9 cells. Nerve growth factor (50 ng/ml, 1.9 nM) induced a 30% decrease in the amount of sphingomyelin in the cells (corresponding to 5.6 pmol per nanomole of phospholipid phosphate) within 12 min (Fig. 3A). Sphingomyelin hydrolysis was maximal (35 to 40% decrease) at NGF concentrations of 100 to 150 ng/ml (Fig. 3B). Activation of SM hydrolysis in the SM cycle should be accompanied by an increase in cellular ceramide levels (*9*). Indeed, NGF (100 ng/ml) also increased the amount of cellular ceramide to a maximum of 1.9 ± 0.2–fold (4.2 ± 0.8 pmol per nanomole of phospholipid phosphate) at 12 min (Fig. 3A). Thus, most of the hydrolyzed SM is accounted for by the generated ceramide. Both SM and ceramide levels recovered to base line within 20 min. This pattern is reminiscent of responses seen with TNF-α in leukemia cells, although NGF produced a greater relative change in SM and ceramide than did TNF-α (*7*). Thus, NGF activates an SM cycle in T9 cells at concentrations approximating the K_d of $p75^{NTR}$ (1 to 4 nM). Moreover, these concentrations correlated closely with those required for process formation (Fig. 2, A and C). On the other hand, NGF (0.26 ng/ml, 10 pM) was sufficient to induce differentiation of PC12 cells (*14*). These results suggest

R. T. Dobrowsky, M. H. Werner, Y. A. Hannun, Departments of Medicine and Cell Biology, Duke University Medical Center, Durham, NC 27710, USA.
A. M. Castellino and M. V. Chao, Department of Cell Biology and Anatomy and Division of Hematology/Oncology, Cornell University Medical College, New York, NY 10021, USA.

*To whom correspondence should be addressed.

that NGF may signal SM hydrolysis through $p75^{NTR}$ in T9 cells.

Although significant process formation and SM hydrolysis were not observed at NGF concentrations below 50 ng/ml, these results do not rule out a role of $p140^{trk}$ in NGF-induced hydrolysis of SM in T9 cells. Therefore, we investigated the expression of NGF receptors by immunoprecipitation and affinity cross-linking. In T9 cells, $p75^{NTR}$ migrated as a broad 70-kD immunoreactive band expressed at levels approximately one-fortieth that seen in PC12 cells (Fig. 4A). The difference in electrophoretic migration of $p75^{NTR}$ for T9 cells compared to that of $p75^{NTR}$ from PC12 cells may arise from differences in the glycosylation of the receptors (*15*). Affinity cross-linking of ^{125}I-labeled NGF with ethylene diamine carbodiimide (EDAC), a reagent that preferentially cross-links $p75^{NTR}$ (*16*), confirmed that $p75^{NTR}$ is expressed in T9 cells, albeit in low amounts relative to that in PC12 cells (Fig. 4B). However, no cross-linking of $p140^{trk}$ was detected in T9 cells, although a 160-kD cross-linked species was detected in fibroblast cells expressing rat $p140^{trk}$ (Fig. 4B) (*16*). Further, Northern (RNA) hybridization of total RNA from T9 cells failed to detect the presence of $p140^{trk}$ transcripts (Fig. 4C). Collectively, this evidence indicates that T9 cells either lack or minimally express $p140^{trk}$, as has been demonstrated in other glioma cell lines (*17*). Thus, these data suggest that NGF-induced ceramide production is mediated by $p75^{NTR}$ in T9 glioma cells.

To exclude further a role for $p140^{trk}$ in NGF-induced sphingomyelin hydrolysis, we examined the effects of NGF in fibroblasts overexpressing $p75^{NTR}$ ($p75^{NTR}$–NIH 3T3 cells) (*18*). Cells of the NIH 3T3 line do not endogenously express either $p140^{trk}$ or $p75^{NTR}$ (*16*). Treatment of $p75^{NTR}$–NIH 3T3 cells with NGF induced a time- and dose-dependent hydrolysis of SM in a manner qualitatively similar to that seen with T9 cells (Fig. 5, A and B). However, NGF treatment of wild-type NIH 3T3 cells showed no decrease in SM concentrations (Fig. 5A). These results indicate that NGF-induced SM hydrolysis is associated with $p75^{NTR}$ and that $p140^{trk}$ is not necessary for this response. Further, human recombinant NGF also induced SM hydrolysis in $p75^{NTR}$–NIH 3T3 cells (*14*). Thus, it is unlikely that the effect of mouse salivary gland NGF on SM hydrolysis is due to a minor impurity in the preparations.

To investigate further the role of $p75^{NTR}$ in NGF-induced hydrolysis of SM, we developed T9 cells that express an epidermal growth factor receptor (EGFR)–$p75^{NTR}$ chimera (*19*, *20*). Epidermal growth factor did not induce SM hydrolysis in wild-type T9 cells (Fig. 6A). Because the EGFR-

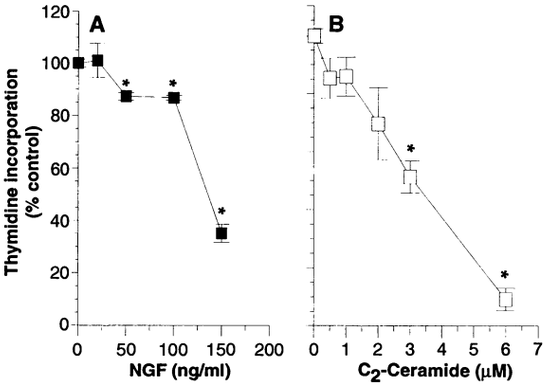

Fig. 1. Effect of NGF and C_2-ceramide on T9 cell growth. Cells were seeded (1×10^3 per well) in DMEM containing 10% BCS and grown overnight. The medium was aspirated, and the cells were washed with PBS and placed in serum-free medium. The cells were treated with (**A**) PBS or NGF for 96 hours or with (**B**) ethanol (0.1%) or C_2-ceramide for 48 hours. Thymidine incorporation was assessed after 6 hours of labeling with [^{3}H]thymidine (1 μCi/ml) (*28*). NGF was added daily, and C_2-ceramide was added only once. Base line thymidine uptake was 15,355 ± 395 or 18,712 ± 352 cpm at 48 and 96 hours, respectively. Results are mean ± SEM from quadruplicate determinations. Asterisks, $p < 0.05$ versus control by Student's *t* test with Bonferroni's multiple comparison correction.

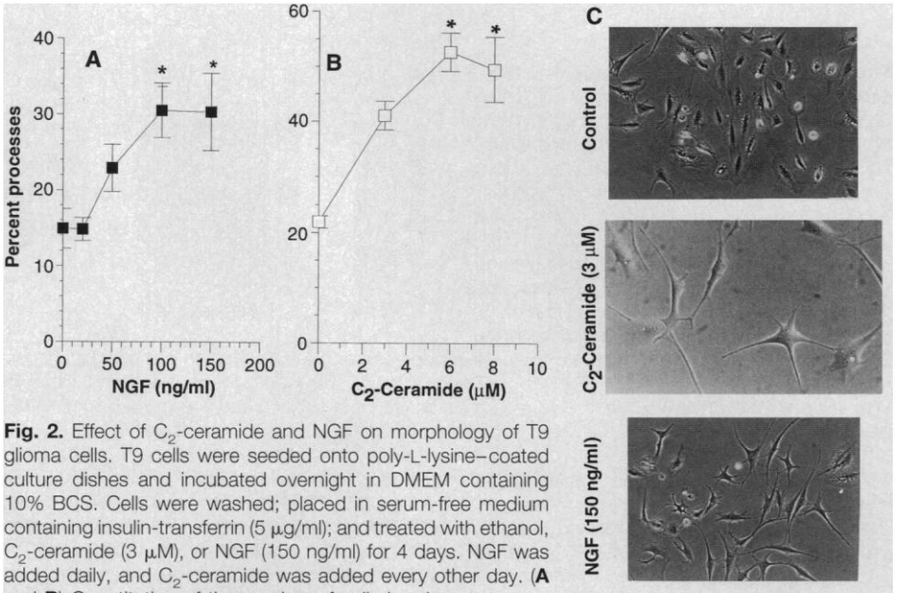

Fig. 2. Effect of C_2-ceramide and NGF on morphology of T9 glioma cells. T9 cells were seeded onto poly-L-lysine–coated culture dishes and incubated overnight in DMEM containing 10% BCS. Cells were washed; placed in serum-free medium containing insulin-transferrin (5 μg/ml); and treated with ethanol, C_2-ceramide (3 μM), or NGF (150 ng/ml) for 4 days. NGF was added daily, and C_2-ceramide was added every other day. (**A** and **B**) Quantitation of the number of cells bearing processes greater than one cell body in diameter from random fields of at least 100 cells. Results are mean ± SEM from quadruplicate determinations. Asterisks, $p < 0.05$ versus control by Student's *t* test with multiple comparison correction. (**C**) Representative field of cells from (A) and (B) photographed under phase-contrast optics.

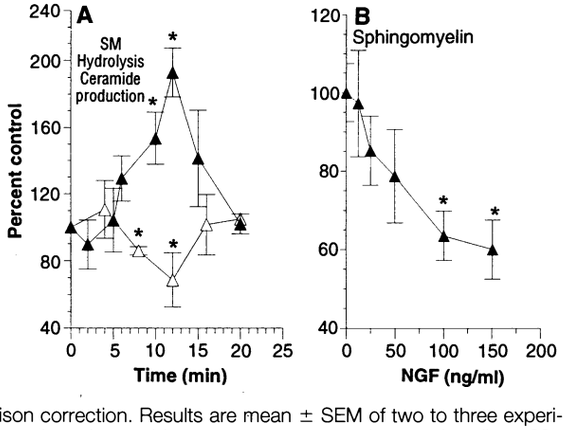

Fig. 3. Induction of SM hydrolysis and ceramide production by NGF in T9 glioma cells. (**A**) Time course of SM hydrolysis (open triangles) and ceramide production (closed triangles) to NGF (50 or 100 ng/ml, respectively). Control SM and ceramide levels were 726 ± 40 cpm per nmol of phosphate and 2.2 ± 0.3 pmol per nmol of phosphate, respectively. Asterisks, $p < 0.05$ versus time-matched control by Student's *t* test. (**B**) Dose response of SM hydrolysis to NGF at 12 min. Control SM level was 1348 ± 99 cpm per nanomole of phosphate. Asterisk, $p < 0.05$ versus control by Student's *t* test with multiple comparison correction. Results are mean ± SEM of two to three experiments performed in triplicate. Sphingomyelin and ceramide measurements were done as described (*29*).

p75^{NTR} chimera contains the transmembrane and cytoplasmic domains of p75^{NTR} but also the ligand binding domain of the EGFR (*19*), activation of SM hydrolysis by EGF in cells expressing this chimera would provide evidence for a role of p75^{NTR} in signaling. In this respect, expression of the EGFR-p75^{NTR} chimera in PC12 cells imparted to EGF the ability to mimic NGF in inducing morphological changes (*19*). In the present study, T9EN10 cells (*20*), which express the EGFR-p75^{NTR} chimera, gave a significant increase in SM hydrolysis in response to treatment with EGF (Fig. 6A). This response was specific for T9EN10 cells and was not observed in the control transfected cell line, T9SV2neo. Epidermal growth factor also increased the amount of ceramide approximately threefold in T9EN10 cells but did not affect the amount of ceramide in wild-type T9 cells (Fig. 6B). Thus, EGF mimicked the effects of NGF on SM hydrolysis and ceramide production in cells expressing the EGFR-p75^{NTR} chimera. These data indicate that activation of the SM cycle is associated with p75^{NTR} and that the presence of the transmembrane and cytoplasmic domains of p75^{NTR} are sufficient to activate the SM cycle. Taken together, the above data provide several lines of evidence indicating that NGF activates the SM cycle specifically through p75^{NTR}.

Two structural roles have been suggested for p75^{NTR}: participation in the formation of a high-affinity NGF binding site (*3*, *18*, *21*) and the binding of neurotrophins for presentation to *trk* receptors (*22*). However, a third potential function for p75^{NTR} is in signal transduction. The finding of protein kinase activities associated with p75^{NTR} (*23*) and the presence of a mastoparan-like G protein binding sequence at the carboxyl terminus of p75^{NTR} (*24*) have implicated a possible involvement of p75^{NTR} in downstream signaling events. Indeed, p75^{NTR} appears to function in the induction of apoptosis, enhancement of developmental cell death in the avian isthmo-optic nucleus, the metastatic progression of primary melanoma, the migration of Schwann cells, and the hydrolysis of glycosyl-phosphatidylinositol (*25*). In glial cells, the internalization of NGF may represent an initial step in a cascade of intracellular effects elicited by p75^{NTR} (*17*).

Our results indicate that p75^{NTR} is coupled to a signal transduction pathway. Ceramide may regulate events during developmental cell death, retrograde transport, and synaptic vesicle fusion as well as maintain

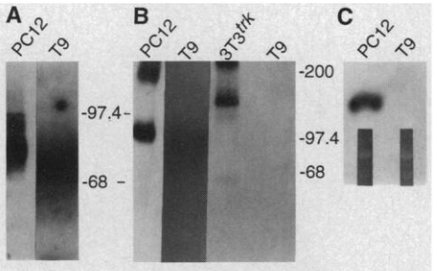

Fig. 4. Expression of p75^{NTR} but not p140^{trk} in T9 cells. (**A**) Protein immunoblot analysis. PC12 cells and T9 cells were grown to confluency and solubilized in 0.5 ml of lysis buffer [100 mM tris-HCl (pH 7.6), 66 mM EDTA, 1% NP-40, 0.4% deoxycholate, 1 mM phenylmethylsulfonyl fluoride, 1 mM leupeptin, and 1 mM aprotinin]. After centrifugation, the supernatant (PC12, 150 μg; T9, 6 mg) was incubated with affinity-purified antibody to p75^{NTR} overnight at 4°C. Protein A–Sepharose (50 μl) was added, and after 2 hours the immunoprecipitate was washed five times in lysis buffer. Proteins were resolved by polyacrylamide gel electrophoresis on 7% gels. Protein immunoblot analysis was done as described (*30*). (**B**) Affinity–cross-linking analysis. Confluent cells were released with PBS containing 1 mM EDTA, washed in PBS, and resuspended in a solution containing 1% bovine serum albumin and 1% glucose (3×10^6 cells per milliliter). The cell suspension was incubated with 0.2 nM ^{125}I-labeled NGF at room temperature for 45 min, and the cross-linking of p75^{NTR} and p140^{trk} was initiated by the addition of either 4 mM EDAC (lanes 1 and 2) for cross-linking of p75^{NTR} or 150 mM disuccinimidyl suberate (lanes 3 and 4) for cross-linking of p140^{trk} (*16*). After 45 min at room temperature, the cells were centrifuged and washed three times with PBS containing 50 mM lysine. The sedimented cells were solubilized in lysis buffer (0.5 ml) at 4°C for 30 min, and the cell debris was sedimented. The supernatant was then subjected to immunoprecipitation and electrophoresis as described. Molecular size markers are indicated in kilodaltons. (**C**) Northern blot analysis. Total RNA was isolated from PC12 and T9 cells and was fractionated on 1% agarose–6.6% formaldehyde gels (30 μg). RNA was transferred to nitrocellulose and hybridized with nick-translated cDNA fragments of p140^{trk}. RNA bands were visualized by autoradiography for 48 hours. Acridine orange staining of the gel is displayed to indicate the relative amounts of RNA loaded.

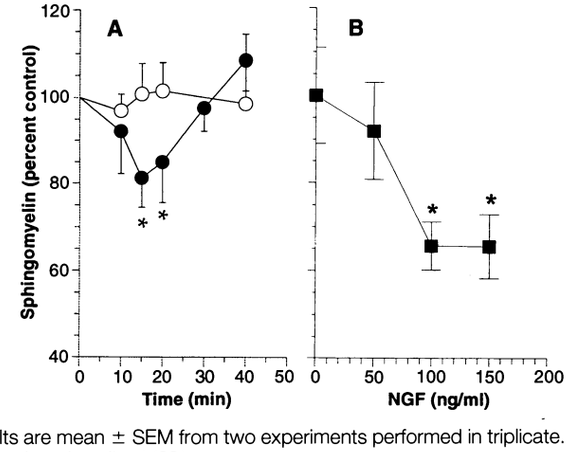

Fig. 5. Activation of the SM cycle by NGF in p75^{NTR}–NIH 3T3 cells. (**A**) Time course of SM hydrolysis to treatment with NGF (100 ng/ml) in wild-type NIH 3T3 cells (open circles) and p75^{NTR}–NIH 3T3 cells (closed circles). Control SM levels were 238 ± 19 and 488 ± 14 cpm per nmol of phosphate in NIH 3T3 and p75–NIH 3T3 cells, respectively. Asterisks, $p < 0.05$ versus time-matched control by Student's *t* test. (**B**) Dose response of SM hydrolysis after treatment with NGF for 15 min in p75^{NTR}–NIH 3T3 cells. Control SM level was 342 ± 38 cpm per nanomole of phosphate. Asterisks, $p < 0.05$ versus control by Student's *t* test with multiple comparison correction. Results are mean ± SEM from two experiments performed in triplicate. Sphingomyelin hydrolysis was measured as described (*29*).

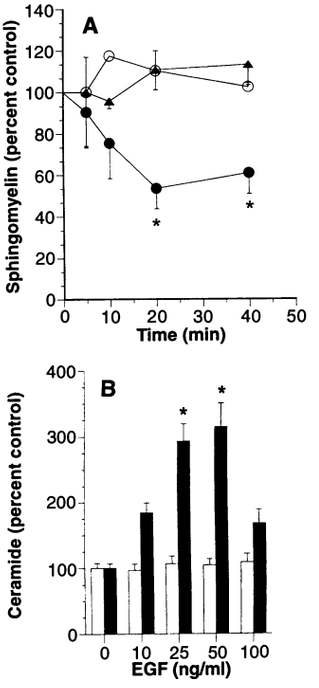

Fig. 6. Activation of the SM cycle by EGF in cells expressing an EGFR-p75^{NTR} chimera. (**A**) Effect of EGF (100 ng/ml) on SM hydrolysis in T9 (open circles), T9EN10 (filled circles), and T9SV2neo (filled triangles) cells. Base line SM levels were 202 ± 14, 277 ± 18, and 557 ± 13 cpm per nanomole of phosphate in T9, T9EN10, and T9SV2neo cells, respectively. Asterisks, $p < 0.05$ versus time-matched control by Student's *t* test. (**B**) Dose dependence of ceramide production in response to treatment with EGF for 20 min in T9 (open bar) and T9EN10 (solid bar) cells. Control ceramide levels were 2.7 ± 0.1 and 9.1 ± 0.6 pmol per nanomole of phosphate in T9 and T9EN10 cells, respectively. Asterisks, $p < 0.05$ versus control by Student's *t* test with multiple comparison correction. Results are means ± SEM of two experiments performed in triplicate. Sphingomyelin hydrolysis and ceramide production were measured as described (*29*).

axonal structure and function. Further, the ability of ceramide to inhibit the growth of T9 cells, which only express $p75^{NTR}$, suggests that the SM cycle may be a prominent signaling pathway in cells primarily expressing $p75^{NTR}$, such as glioma, schwannoma (*17*), and melanoma cells (*25*) or cells overexpressing $p75^{NTR}$ in response to axotomy or senile dementia (*26*). The antiproliferative and differentiative effects of ceramide may occur by modulation of cellular protein phosphorylation and the down-regulation of the c-myc proto-oncogene (*7*). Both a ceramide-activated kinase (*7*, *8*) and phosphatase (*27*) have been identified that may provide direct molecular targets for further downstream effects of ceramide (*10*).

REFERENCES AND NOTES

1. R. Levi-Montalcini, *Science* **237**, 1154 (1987).
2. R. Klein, S. Jing, V. Nanduri, E. O'Rourke, M. Barbacid, *Cell* **65**, 189 (1991).
3. B. L. Hempstead, D. Martin-Zanca, D. R. Kaplan, L. F. Parada, M. V. Chao, *Nature* **350**, 678 (1991).
4. M. J. Radeke, T. P. Misko, C. Hsu, L. A. Herzenberg, E. M. Shooter, *ibid.* **325**, 593 (1987); D. Johnson *et al.*, *Cell* **47**, 545 (1986).
5. A. Rodriguez-Tebar, G. Dechant, R. Gotz, Y.-A. Barde, *EMBO J.* **11**, 917 (1992).
6. S. J. Birren, J. M. Verdi, D. J. Anderson, *Science* **257**, 395 (1992); C. Cordon-Cardo *et al.*, *Cell* **66**, 173 (1991).
7. L. M. Obeid, C. M. Linardic, L. A. Karolak, Y. A. Hannun, *Science* **259**, 1769 (1993); M. Kim, C. Linardic, L. Obeid, Y. Hannun, *J. Biol. Chem.* **266**, 484 (1991); S. Mathias, K. A. Dressler, R. N. Kolesnick, *Proc. Natl. Acad. Sci. U.S.A.* **88**, 10009 (1991).
8. L. R. Ballou, C. P. Chao, M. A. Holness, S. C. Barker, R. Raghow, *J. Biol. Chem.* **267**, 20044 (1992); S. Mathias *et al.*, *Science* **259**, 519 (1993).
9. T. O. Okazaki, R. M. Bell, Y. A. Hannun, *J. Biol. Chem.* **264**, 19076 (1989).
10. Y. A. Hannun and C. M. Linardic, *Biochem. Biophys. Acta* **1154**, 223 (1994).
11. C. A. Smith, T. Farrah, R. G. Goodwin, *Cell* **76**, 959 (1994).
12. Y. Marushige, N. R. Raju, K. Marushige, A. Koestner, *Cancer Res.* **47**, 4109 (1987).
13. T. O. Okazaki, A. Bielawska, R. M. Bell, Y. A. Hannun, *J. Biol. Chem.* **265**, 15823 (1990).
14. R. T. Dobrowsky and Y. A. Hannun, unpublished observations.
15. P. M. Grob, A. H. Ross, H. Koprowski, M. Bothwell, *J. Biol. Chem.* **260**, 8044 (1985).
16. S. O. Meakin and E. M. Shooter, *Neuron* **6**, 153 (1991); D. R. Kaplan, B. L. Hempstead, D. Martin-Zanca, M. V. Chao, L. F. Parada, *Science* **252**, 554 (1991).
17. P. Kahle and C. Hertel, *J. Biol. Chem.* **267**, 13917 (1992).
18. D. Mahadeo, L. Kaplan, M. V. Chao, B. L. Hempstead, *ibid.* **269**, 6884 (1994).
19. H. Yan, J. Schlessinger, M. V. Chao, *Science* **252**, 561 (1991).
20. Rat T9 cells were transfected by the calcium phosphate precipitation method with 1 μg of pCMVEN10 complementary DNA (cDNA) (*19*) and 0.1 μg of *pSV2neo* (neomycin resistance gene). Transfection with *pSV2neo* only served as the control. Twenty-four hours after transfection, cells were placed in Dulbecco's modified Eagle's medium (DMEM) containing 10% bovine calf serum (BCS) and G418 (0.6 mg/ml). After 2 to 3 weeks, neomycin-resistant colonies were pooled and subcultured in DMEM containing 10% BCS and G418 (0.25 mg/ml) for use in all subsequent experiments. Cells were designated T9EN10 and T9SV2neo. To examine integration of chimeric cDNA, genomic DNA was isolated and Southern blot analysis was performed. The pooling of stable colonies avoids the bias associated with the analysis of single colonies and, therefore, is representative of clones expressing various amounts of receptor.
21. B. L. Hempstead, N. Patil, B. Thiel, M. V. Chao, *J. Biol. Chem.* **265**, 9595 (1990).
22. S. Jing, P. Tapley, M. Barbacid, *Neuron* **9**, 1067 (1992).
23. M. Ohmichi, S. Decker, A. R. Saltiel, *Cell Reg.* **2**, 691 (1991); C. Volonte, J. M. Angelastro, L. A. Greene, *J. Biol. Chem.* **268**, 21410 (1993).
24. D. Feinstein and D. Larhammer, *FEBS Lett.* **272**, 7 (1990).
25. S. Rabizadeh *et al.*, *Science* **261**, 345 (1993); G. L. Barrett and P. Bartlett, *Proc. Natl. Acad. Sci. U.S.A.* **91**, 6501 (1994). C. S. von Bartheld *et al.*, *Neuron* **12**, 639 (1994); J. L. Herrmann *et al.*, *Mol. Biol. Cell* **4**, 1205 (1993); J. Represa *et al.*, *Proc. Natl. Acad. Sci. U.S.A.* **88**, 8016 (1991); E. S. Anton, G. Weskamp, L. F. Reichardt, W. D. Matthew, *ibid.* **91**, 2795 (1994).
26. M. Taniuchi, H. B. Clark, J. B. Schweitzer, E. M. Johnson, *J. Neurosci.* **8**, 664 (1988); P. Ernfors, N. Lindefors, V. Chan-Palay, H. Persson, *Dementia* **1**, 138 (1990).
27. R. T. Dobrowsky and Y. A. Hannun, *J. Biol. Chem.* **267**, 5048 (1992); R. T. Dobrowsky, C. Kamibayashi, M. C. Mumby, Y. A. Hannun, *ibid.* **268**, 15523 (1993).
28. A. Olivera, N. E. Buckley, S. Spiegel, *ibid.* **267**, 26121 (1992).
29. Rat T9 cellls were grown for 72 hours in the presence of [^{3}H]choline (0.5 μCi/ml, 86 Ci/mmol) in DMEM containing 10% BCS. The medium was removed, and the cells were washed with phosphate-buffered saline (PBS) and incubated in serum-free DMEM containing 25 mM Hepes (pH 7.4) for 4 to 6 hours before treatment. Cells were treated with either PBS or mouse 2.5S NGF in PBS (Harlan Bioproducts for Science) at 37°C for the indicated times, the medium was aspirated, and the cells were fixed with 2 ml of methanol. Lipids were extracted and the amount of SM was quantitated by resuspending 10 to 15 nmol of total lipid phosphorous in 50 μl of 200 mM tris-HCl (pH 7.4), 10 mM $MgCl_2$, and 1% Triton X-100. Reactions were initiated by the addition of 50 μl of 10 mM tris-HCl (pH 7.4) containing 100 mU of bacterial sphingomyelinase (*Streptomyces* sp., Sigma), and the mixture was incubated for 2 hours at 37°C. The reaction was terminated by the addition of 1.5 ml of chloroform:methanol (2:1, v/v). Hydrolyzed [^{3}H]phosphocholine was recovered in the aqueous phase after the addition of 0.2 ml of water. The amount of [^{3}H]phosphocholine released was normalized to total phospholipid mass [S. Jayadev, C. M. Linardic, Y. A. Hannun, *J. Biol. Chem.* **269**, 5757 (1994)]. Ceramide mass was quantitated as described [P. P. VanVeldhoven, D. P. Matthews, D. P. Bolognesi, R. M. Bell, *Biochem. Biophys. Res. Commun.* **187**, 209 (1992)].
30. M. Benedetti, A. Levi, M. V. Chao, *Proc. Natl. Acad. Sci. U.S.A.* **90**, 7859 (1993).

31. We thank D. Mahadeo for help in affinity cross-linking and A. Bielawska for synthesizing C_2-ceramide. Supported in part by National Institutes of Health (NIH) grant GM43825 and a scholarship from the PEW Foundation. Y.A.H. is a Mallinkrodt Scholar. M.V.C. is supported by the National Institutes of Health, a Zenith Award from the Alzheimer's Association, and the Dorothy Rodbell Cohen Foundation. R.T.D. is recipient of National Research Service Award AG05531. M.H.W. was an Andrea Rhodes Fellow of the American Brain Tumor Association. A.M.C. is an Aaron Diamond Foundation Fellow, and this work was supported in part by a grant from the Aaron Diamond Foundation.

8 February 1994; accepted 8 July 1994

TECHNICAL COMMENTS

Entropic Elasticity of λ-Phage DNA

DNA is unique among polymers both for its size, and for its long persistence length, $A \approx 50$ nm (*1*). Since A encompasses many base pairs, and thus to a large degree is averaged over sequence, a continuum elastic description of DNA bending is plausible. Recently, S. B. Smith *et al.* made a direct mechanical measurement of the force versus extension $F(x)$ for a 97-kb λ-DNA dimer (*2*). Here we show that these experimental data may be precisely fit by the result of an appropriate elastic theory and thereby provide a quantitative baseline, departures from which will signal effects of more biological interest.

If the force is used as a Lagrange multiplier to fix the extension, the free energy of a stretched worm-like polymer corresponds to the quantum-mechanical ground state energy of a dipolar rotator with moment of inertia A, subject to an electric field F (*3*). Although the quality of the experimental data required us to supply a complete numerical solution, both the large- and small-force limits admit analytical asymptotic solutions that are summarized by the following interpolation formula:

$$FA/kT = \frac{1}{4}(1 - x/L)^{-2} - \frac{1}{4} + x/L$$

where k is Boltzmann's constant, T is temperature, and L is the molecular contour length. For large $F \gg kT/A$, the accessible conformations reduce to quadratic fluctuations around a straight line, while for $F \ll kT/A$ the polymer conformation becomes a directed random walk. The force needed to extend a freely jointed chain model diverges less strongly as $x \to L$ [$F \propto (1 - x/L)^{-1}$] as fluctuations inside each segment are suppressed.

A nonlinear least-squares fit of the exact $F(x)$ to experimental data (Fig. 1) gives $L = 32.80 \pm 0.10$ μm and $A = 53.4 \pm 2.3$ nm (90% confidence level errors; $\chi^2/n = 1.04$ for $n = 303$ data points). This L is close to the crystallographic value of 32.7 μm, while A is in good agreement with the results of cyclization studies (*1*). Refinements of the present technique may well become the most accu-